

## Effect of Thermal Treatment on $\text{AlO}_x/\text{Co}_{90}\text{Fe}_{10}$ Interface of Magnetic Tunnel Junctions Prepared by Radical Oxidation

Donkoun Lee, Jangsik In, and Jongill Hong\*

Ceramic Engineering, Advanced Materials Engineering, Yonsei University, 134 Shinchon, Seodaemun, Seoul 120-749, Korea

(Received 1 October 2005)

We confirmed that the improvement in properties of magnetic tunnel junctions prepared by radical oxidation after thermal treatment was mostly resulted from the redistribution of oxygen at the  $\text{AlO}_x/\text{Co}_{90}\text{Fe}_{10}$  interface. The as-deposited Al oxide barrier was oxygen-deficient but most of it re-oxidized into  $\text{Al}_2\text{O}_3$ , the thermodynamically stable stoichiometric phase, through thermal treatment. As a result, the effective barrier height was increased from 1.52 eV to 2.27 eV. On the other hand, the effective barrier width was decreased from 8.2 Å to 7.5 Å. X-ray absorption spectra of Fe and Co clearly showed that the oxygen in the CoFe layer diffused back into the Al barrier and thereby enriched the barrier to close to a stoichiometric  $\text{Al}_2\text{O}_3$  phase. The oxygen bonded with Co and Fe diffused back by 6.8 Å and 4.5 Å after thermal treatment, respectively. Our results confirm that controlling the chemical structures of the interface is important to improve the properties of magnetic tunnel junctions.

**Key words :** tunneling magnetoresistance, Fe oxide, Co oxide,  $\text{Al}_2\text{O}_3$  barrier, x-ray absorption spectroscopy, chemical fine structure

### 1. Introduction

Magnetic tunnel junctions (MTJs) become promising candidates for electronic applications, such as magnetic read sensors and non-volatile memory elements, due to their high values of tunneling magnetoresistance (TMR) at room temperature [1]. Until now substantial effort has been made on issues of how to improve the structures and materials of MTJs with good enough electrical and magnetic properties for such devices. In particular, obtaining Al-oxide tunnel barrier with being pin-hole free and very smooth is one of major issues because the quality of the barrier is critical to improve the electrical and magnetic properties of MTJs. Various oxidation methods, such as natural oxidation [2] and plasma oxidation [3], have been explored to fabricate such a barrier of high quality. Among those methods, plasma oxidation has been popular because it has required less oxidation time and produced strong oxide barriers as well [3]. However, recent report suggested that the large TMR could also be achieved by the barrier prepared by a radical oxidation method which energetically weak oxygen radicals are dominant in the

process of. Therefore, radical oxidation can be considered as another good way to oxidize the metal barrier, especially when the barrier is ultra-thin [4].

On the other hand, appropriate annealing process has been necessary to enhance the properties of MTJs [5, 6]. Though many researchers have succeeded in improving the properties of MTJs by thermal treatment, they could not yet provide crystal-clear explanations of the effect of thermal treatment on such improvement. Previous analyses including Rutherford backscattering spectroscopy (RBS) could not clearly identify the chemical fine structures of the interface between the oxide barrier and the underlying magnetic layer due to lack of depth resolution [7]. In this paper, we discuss and explain the effect of thermal treatment on the properties of MTJs prepared by radical oxidation on the basis of chemical fine structures obtained by near-edge x-ray absorption fine structures (NEXAFS) spectroscopy and x-ray photoelectron spectroscopy (XPS).

### 2. Experiment

We prepared two kinds of films in an ultrahigh-vacuum sputtering system: (1) Si substrate/ $\text{SiO}_2$  200/Ta 5/NiFe 2/PtMn 15/CoFe 1.8/Ru 0.9/CoFe 2.8/Al 1/oxidation/CoFe 1.5/NiFe 3/Ta 10 (nm) for MTJs and (2) Si substrate/ $\text{SiO}_2$

\*Corresponding author: Tel: +82-2-2123-5846,  
Fax: +82-2-365-5882, e-mail: hong.jongill@yonsei.ac.kr

200/Ta 5/Cu 10/CoFe 3/Al 1/oxidation/Ta 4 (nm) for chemical analyses, where CoFe and NiFe indicate  $\text{Co}_{90}\text{Fe}_{10}$ , and  $\text{Ni}_{80}\text{Fe}_{20}$ , respectively. For chemical analyses, we modified the sample structure as described elsewhere [8]. The base pressure of the deposition chamber was less than  $3.0 \times 10^{-7}$  Pa and a magnetic field of  $\sim 150$  Oe was applied to induce the uniaxial anisotropy during the deposition. All the films were annealed at a temperature of  $270^\circ\text{C}$  for 5 h under a field of 8 kOe at a pressure of less than  $5.0 \times 10^{-5}$  Pa. The MTJ was fabricated by photo lithography and its junction size was  $30 \times 30 \mu\text{m}^2$ . Radio frequency (RF) power was applied to generate oxygen radicals in a separate oxidation chamber. An Al grid was set up between the source and the film, and it was grounded to reduce the flux of energetic oxygen ions [4]. The applied power was 500 W and the oxygen pressure was 1.5 Pa. We changed the oxidation time to obtain the optimal electrical and magnetic properties of the MTJs. As shown in Fig. 1, our optimization occurred at 180 s for the radical oxidation. We measured the electrical and magnetic properties of the MTJs in the field range of  $-10 \sim 10$  KOe by a four-point probe at room temperature.

We investigated the chemical states of the Al oxide barrier by XPS using a monochromated Al  $K\alpha$  source at 1487 eV. The base pressure of the experimental chamber was less than  $3.0 \times 10^{-7}$  Pa. To increase the signal for XPS, we etched the 4 nm-thick Ta cap with 1% of HF for 100 s just before loading the films into the experimental chamber because the Ta was too thick to detect signals from the interface. Optimization of the wet etching condition can be found in [8]. To study the chemical structures of the interface, we carried out NEXAFS measurements for the  $L$ -edges of Co and Fe on the U7 beamline at the Pohang Light Source, which provides a highly brilliant and monochromatic linear-polarized soft x-ray for high-resolution spectroscopy. The  $L$ -edges x-ray absorption spectra (XAS) of Co and Fe are mainly originated from transitions between  $2p$ - and  $3d$ -dipoles, and they are extremely sensitive to oxidation states, spin states, and bond covalency. We took the  $L$ -edge XAS of Fe and Co in a total electron yield (TEY) mode, recording the sample drain current. The base pressure of the experimental chamber was less than  $5.0 \times 10^{-7}$  Pa. The absolute energies of the  $L$ -edges were calibrated by referencing the spectra of pure metals to those reported [9]. We scanned the NEXAFS spectra with a step size of 0.1 eV.

### 3. Result and Discussion

Figure 1 shows the TMR values of the MTJ prepared by radical oxidation after thermal treatment at  $270^\circ\text{C}$  for 5

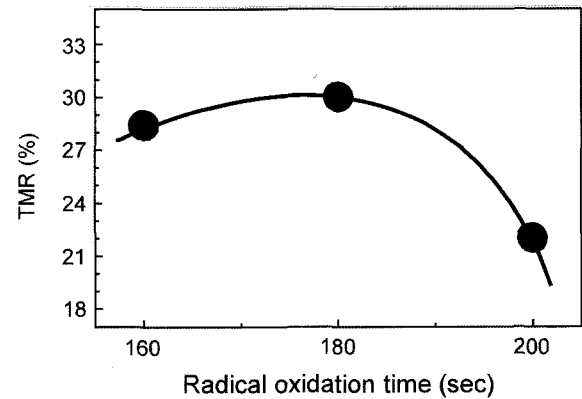


Fig. 1. Variations of TMR values with oxidation time. (The solid curve is a guide to eyes)

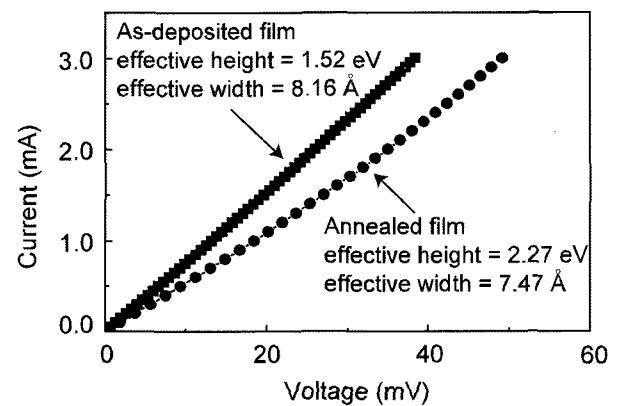


Fig. 2. Current vs. Voltage ( $I$ - $V$ ) for (a) the as-deposited and (b) the annealed MTJ.

h. The TMR value and exchange bias field ( $H_{\text{ex}}$ ) of the annealed MTJ were optimized at 30% and 943 Oe, respectively. To investigate what happened to the barrier of the junctions during the thermal treatment, we measured current vs. voltage ( $I$ - $V$ ) at a field of 10 KOe. The effective barrier height and width for the junctions were estimated by the Simmons theory [10] as shown in Fig. 2. The effective barrier height and width of the as-deposited MTJ were 1.52 eV and 8.2 Å, respectively. As expected, the thermal treatment increased the barrier height to 2.27 eV and decreased the barrier width to 7.5 Å. Those changes can be explained by considering the behavior of oxygen reacted with the barrier and the underlying magnetic layer. In particular, we focused our studies on two possibilities; (1) the re-oxidation of a poorly oxidized phase  $\text{AlO}_x$  and (2) the reduction of Co and Fe oxides in the underlying CoFe layer.

First of all, we analyzed the chemical structure of the Al-oxide barrier itself by XPS for the as-deposited and the annealed film. The chemical structures of the two

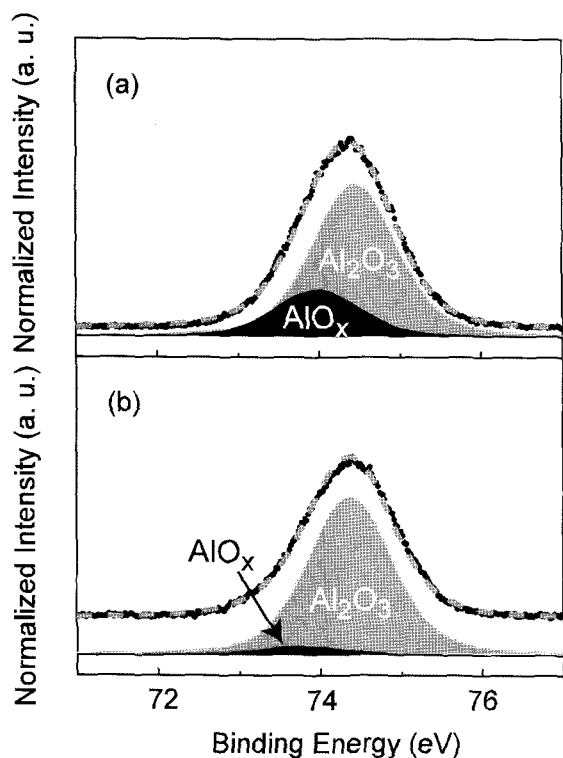


Fig. 3. Al 2*p* XPS spectra of (a) the as-deposited and (b) the annealed film with curve-fitting.

barriers were quite different from each other. Figure 3 shows the Al 2*p* XPS spectra of the as-deposited and the annealed film with curve-fitting, respectively. The peak of metal Al at 73.0 eV [11] shifted to 74.4 eV for Al<sub>2</sub>O<sub>3</sub> [11], and to 73.8 eV for AlO<sub>x</sub>, an oxygen-deficient phase. [12] The background in the curves was corrected by removing the Shirley step [13]. The results reveal that the metal Al was oxidized to both Al<sub>2</sub>O<sub>3</sub> and AlO<sub>x</sub>, and the fraction of each phase in the barrier was significantly changed before and after thermal treatment. In the as-deposited MTJ, the Al<sub>2</sub>O<sub>3</sub> and AlO<sub>x</sub> phases were 81% and 19%, respectively. On the other hand, the thermal treatment helped increase the population of the Al<sub>2</sub>O<sub>3</sub> phase to 97%. In other words, the oxygen-deficient AlO<sub>x</sub> was re-oxidized further during the thermal treatment, which moved the stoichiometry of the barrier closer to Al<sub>2</sub>O<sub>3</sub>. Thus, the diffusion of oxygen from the underlying CoFe layer into the barrier is likely responsible for such enrichment of oxygen, which is described below.

Now, we investigated the chemical structures of the Co and Fe at the interface between the barrier and the underlying CoFe layer. To study the chemical structures of the interface, we conducted NEXAFS experiments for the *L*-edges of Co and Fe. Figures 4(a) and 4(b) show Co *L*<sub>III</sub>-edge XAS of the as-deposited and the annealed film.

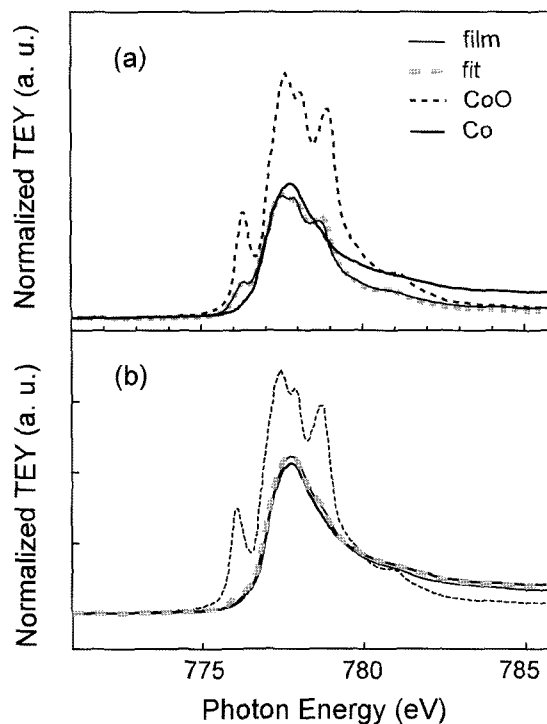


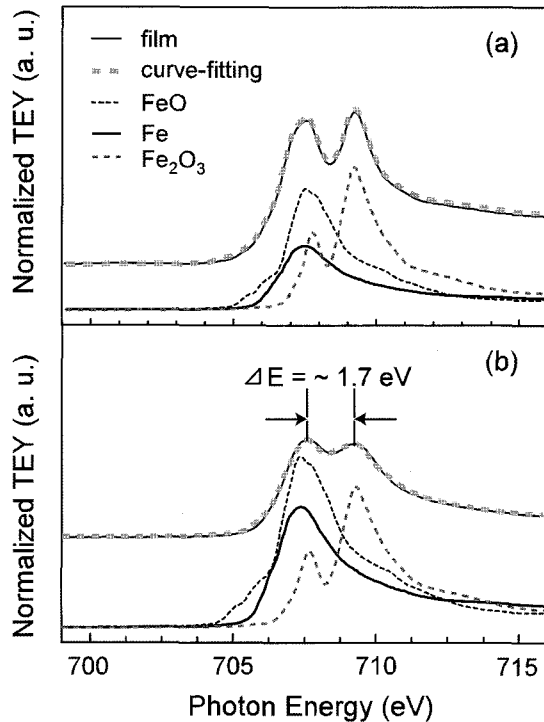
Fig. 4. Co *L*-edge XAS of (a) the as-deposited and (b) the annealed film with curve-fitting.

The curve-fittings based on the bilayer model [14] were also shown in the figure. The *L*<sub>III</sub>-edge spectra of Co at the interfaces show much difference between the as-deposited and annealed films, suggesting Co oxide was reduced to Co by thermal treatment. The multiplet structure of the Co spectra due to the orbital hybridization of O 2*p*- and Co 3*d*-valence indicates that during the oxidation of the barrier, Co was unavoidably attacked by oxygen. The results of curve-fitting showed that the Co in the CoFe layer had a mixture of pure Co and CoO in both cases. However, the curve-fitted thickness of CoO turned out to be decreased much after thermal treatment: 9.1 Å for the as-deposited film and 2.3 Å for the annealed film, respectively. Considering the volume expansion of the CoO (that is, 1 Å of Co corresponds to 1.75 Å of CoO) [14], we could calculate that, in the case of the as-deposited film, 2.6 mono-layers of pure Co were oxidized to CoO. In the case of the annealed film, a 0.6 monolayer of Co was calculated to be oxidized at the interface. This means that only the Co just at the interface may be bonded with the oxygen of the Al<sub>2</sub>O<sub>3</sub> barrier. The chemical structure of the Co clearly shows that the oxygen reacted with the metal Co in CoFe layer diffused back to the barrier during the thermal treatment. The results of the curve-fitting are listed in Table 1.

The chemical structures of the Fe at the interface were

**Table 1.** Curve-fitted results for the Fe and Co  $L_{\text{III}}$ -edge spectra of the as-deposited and annealed MTJs.

		Fe $L_{\text{III}}$ -edge		Co $L_{\text{III}}$ -edge
		FeO	$\alpha\text{-Fe}_2\text{O}_3$	CoO
As-deposited	Fraction	55%	45%	100%
MTJ	Thickness	9.3 Å	9.3 Å	9.1 Å
Annealed	Fraction	36%	64%	100%
MTJ	thickness	4.8 Å	4.8 Å	2.3 Å

**Fig. 5.** Fe  $L$ -edge XAS of (a) the as-deposited and (b) the annealed film with curve-fitting.

changed much before and after the thermal treatment, as shown in Fig. 5. The energy difference between the maximum and the right shoulder peaks of  $L_{\text{III}}$ -edge spectrum,  $E$ , was  $\sim 1.7$  eV. The right shoulder peak has been known to come mainly from  $\alpha\text{-Fe}_2\text{O}_3$  [14]. The detailed curve-fitting based on the bilayer model [14], shows that the Fe was partially oxidized to a mixture of FeO and  $\alpha\text{-Fe}_2\text{O}_3$  phases at the interface and the fraction and thickness of each phase at the interface were significantly different. The curve-fitted thickness of the Fe oxide layer was much different: 9.3 Å for the as-deposited film and 4.8 Å for the annealed film. Thus, in the case of the as-deposited film, about 2.3 monolayers of Fe were oxidized to FeO and  $\alpha\text{-Fe}_2\text{O}_3$ . On the other hand, the thermal treatment helped reduce a 1.0 monolayer of

Fe at the interface because the oxidation of 1-thick Fe transforms into 1.78 Å-thick FeO and 2.14 Å-thick  $\alpha\text{-Fe}_2\text{O}_3$  [14]. The Fe  $L_{\text{III}}$ -edge XAS clearly show that most oxygen reacted with the Fe diffused back to the barrier during the thermal treatment. Consequently, mostly metal Fe has remained at the interface.

Our analyses confirm that the oxygen, upon having reacted with the Co and Fe, indeed diffused back to the barrier and contributed to the enrichment of the Al oxide barrier through thermal treatment, which explains the origin of an increase in the effective tunneling barrier height. The stoichiometric  $\text{Al}_2\text{O}_3$  is expected to have fewer trapping sites and to be more homogeneous than the oxygen-deficient  $\text{AlO}_x$ , and thus the former has the tunneling barrier height higher than the latter [15]. These results are consistent with a thermodynamic consideration which predicts that the mixing enthalpy of  $\text{Al}_2\text{O}_3$  has larger than that of Fe and Co;  $\text{Al}_2\text{O}_3$ :  $-1583.0 \times 10^{-3}$  J/mole, FeO:  $-245.6 \times 10^{-3}$  J/mole,  $\alpha\text{-Fe}_2\text{O}_3$ :  $-742.8 \times 10^{-3}$  J/mole, CoO:  $-216.5 \times 10^{-3}$  J/mole [14]. In other words, Al is a stronger reducing agent than Fe and Co. The reduction of Co and Fe oxides can also explain in part the decrease in the effective barrier width.

An interesting thing to note is that the population of Fe oxide phase was quite different between the as-deposited and the after-being-annealed films. In the case of the as-deposited film, the fraction of the FeO and  $\alpha\text{-Fe}_2\text{O}_3$  was 55% and 45%, respectively. On the other hand, the thermal treatment increased the fraction of the  $\alpha\text{-Fe}_2\text{O}_3$  to 64%, as listed in Table 1. That is, most Fe oxide phases were transformed into the most thermodynamically stable phase  $\alpha\text{-Fe}_2\text{O}_3$  through the thermal treatment, which has been confirmed by our previous study [16].

#### 4. Conclusion

In conclusion, we have shown that the chemical structure at the interface between the barrier and the underlying CoFe layer was significantly affected by the thermal treatment; (1) In the study of NEXAFS and XPS, the underlying Co and Fe oxides were reduced to metal Co and Fe, and (2) most of the  $\text{AlO}_x$  barrier was re-oxidized to  $\text{Al}_2\text{O}_3$  by oxygen diffused from the underlying Co and Fe oxides during the thermal treatment. Those changes can be the origins of the increase in the effective barrier height and the decrease in the effective barrier width of MTJs when they are prepared by the radical oxidation and thermal treatment. Our results confirm that controlling the chemical structures of the interface is important to improve the properties of magnetic tunnel junctions.

## Acknowledgement

This work was supported by The Korea Research Foundation Grant funded by the Korean Government (MOEHRD) (KRF-2003-041-D20252). Authors gratefully acknowledge T. J. Regan for fitting of XAS.

## References

- [1] S. Tehrani, J. M. Slaughter, E. Chen, M. Durlam, J. Shi, and M. Deherrera, *IEEE Trans. Magn.* **35**, 2814 (1999).
- [2] H. Tsuge, and T. Mitsuzuka, *Appl. Phys. Lett.* **71**, 3296 (1997).
- [3] J. S. Moodera, L. R. Kinder, T. M. Wang, and R. Meservey, *Phys. Rev. Lett.* **74**, 3273 (1995).
- [4] M. Tsunoda, K. Nishikawa, S. Ogata, and M. Takahashi, *Appl. Phys. Lett.* **80**(17), 3135 (2002); K. Shimazawa, N. Kasahara, J. J. Sun, S. Araki, H. Morita, and S. H. Matuszaki, *J. Appl. Phys.* **87**(9), 5194 (2000).
- [5] R. C. Sousa, J. J. Sun, V. Soares, P. P. Freitas, A. Kling, M. F. da Silva, and J. C. Soares, *Appl. Phys. Lett.* **73**, 3288 (1998).
- [6] Z. Zhang, S. Cardoso, P. P. Freitas, P. Wei, N. Barradas, and J. C. Soares, *Appl. Phys. Lett.* **78**, 2911 (2001).
- [7] X. Batlle, P. J. Cuadra, Zhongzhi Zhang, S. Cardoso, P. P. Freitas, *J. Magn. Magn. Mater.* **261**, L305 (2003).
- [8] D. Lee and J. Hong, *J. Appl. Phys.* **97**, 093905 (2005).
- [9] J. G. Chen, *Surf. Sci. Rep.* **30**, 1 (1997).
- [10] J. G. Simmons, *J. Appl. Phys.* **34**(6), 1793 (1963).
- [11] J. Chastain, *Handbook of X-ray Photoelectron Spectroscopy* (Perkin-Elmer Corporation, 1992).
- [12] X. Batlle, B. J. Hattink, A. Labarta, J. J. Akerman, R. Escudero, and I. K. Schuller, *J. Appl. Phys.* **91**, 10163 (2002).
- [13] D. A. Shirley, *Phys. Rev. B* **5**, 4709 (1972).
- [14] T. J. Regan, H. Ohldag, C. Stamm, F. Nolting, J. Lüning, J. Stöhr, and R. L. White, *Phys. Rev. B* **64**, 214422 (2001).
- [15] J. Zhang and R. M. White, *J. Appl. Phys.* **83**(11), 6512 (1998).
- [16] J. Hong, Y. Lee, M. K. Lee, H. J. Song, H. Shin, Y. Yoo, and J. Suh, *Appl. Phys. Lett.* **83**, 4803 (2004).